

Using UWB Sensor for Delta Robot Vibration Detection

Jyun-Long Chen¹, Tien-Cheng Tseng², Yu-Yi Cheng³, Kuang-I Chang⁴, Jwu-Sheng Hu⁵

^{1,2,3,4} Center for Measurement Standards, Industrial Technology Research Institute

⁵ Mechanical and Systems Research Laboratories, Industrial Technology Research Institute

Abstract— This study proposed the ultra-wideband(UWB) sensor to detect the vibration of the delta robot and the distance between UWB sensor and robot arm. Based on the radar propagating principle and the proposed algorithm, the vibration status of robot arm can be obtained. Besides, the vibration status can be reduced by feedback the information to the controller of the robot arm. The advantage of the proposed sensor is that without contacting to the robot arm, UWB sensor is more flexible to be used and will not cause any unnecessary payload as accelerometers. With proper calibration, the simulation of vibration frequency and the real-time absolute position of the robot arm were calculated and demonstrated. The experimental results show that the correlations for measured frequency and distance approximate to 1.

I. INTRODUCTION

Along with increase of labor cost and progress of automation technology, robot arms were proposed to be used for manufacturing and assembling, so as to improve human throughput and product quality. In view of a present situation, in a production process of an intelligent automation system, a fast operation speed is mainly considered. The linear Delta robots were suggested to deal with fast assembling like pick-and-place or any other applications needing speed, forces and stiffness [1]. However, this robot arm subjected to high acceleration and structural flexibility would lead to unwanted structural vibration during operation [2]. In order to reduce the residual vibration of robots, Park *et al.* proposed a practical design and application of time-varying input shaping technique to deal with it [3]. Harada *et al.* proposed a control method using a pattern generator and a reinforcement learning algorithm [4]. Furuta *et al.* [5] as well as Xing *et al.* [6] used a mathematic model and effectively reduced the system vibration. A few of studies [7]-[9] proposed to monitor the vibrations by using accelerometers. However, considering the light payload, the accelerometer belongs to an embedded sensing device, which has more limitations in applications. Except accelerometers, the vibration can be detected by laser vibrometers. However, laser vibrometers are very expensive. We proposed a novel ultra-wideband (UWB) sensor which was used to detect human heartbeat [10]. Under this principle, vibration signals as well as distance would be detected and analyzed to reduce the vibration of robot arms. The nature of non-contact measurement makes UWB a strong candidate to measure vibration during robot operation. Extensive

experiments have been conducted to evaluate the effect of vibration measurement. Take delta robot as an example, it operates in a restricted area. An UWB can be installed in a fixed location. Careful adjustment ensures the UWB signal aiming to the specific location on the robot, and thus the vibration of that location being measured. What makes it stand out from conventional accelerometers is that it is able to measure the vibration profile of the entire robot, which requires multiple accelerometers to complete the same task. The vibration profile is defined as the vibration of each section of the robot, not the end-effector that only exhibits the vibration summation of the whole robot. It helps to identify any undesired vibration during operation. By arranging the antenna array in an UWB sensor, the reading from the array can be mapped to the vibration profile of the robot. Furthermore, the positioning capability of the UWB sensor can feed back the absolute position of the end-effector to help the robot achieve better position accuracy.

II. RADAR SYSTEM PRINCIPLES AND ARCHITECTURE

A. Theory of operation

Consider Fig. 1, when the object is moving, the measurement of UWB signal carrying useful information is performed through evaluation of a phase difference between the reference probing signal and the signal reflected from the investigated subject.

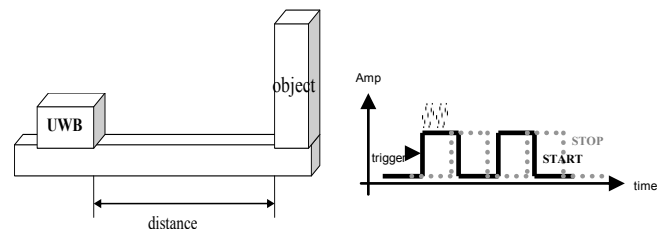


Figure 1. Reference probing signal and the signal reflected diagram

In conventional signal processing a correlation processing system is utilized. The functioning of such systems is based on multiplication of the reference probing signal and the return signal delayed by the time interval during which the signal is spread to the investigated subject and back to the receiving antenna. The probing signal is presented in the form of short radio pulses having duration not in the excess of a period of

oscillations filling the probing pulse. The output signal of a correlation system is proportional to the phase difference between the probing signal and the return signal.

The amplitude Z of the output signal after processing is characterized by the following ratio:

$$Z = (E_0 E_1) / 2 \times n T_0 \cos(u) \quad (1)$$

where E_0 is a maximum amplitude of the probing signal; E_1 is a maximum amplitude of the received return signal; T_0 is a period of oscillations of the probing signal; n is a whole number of periods of oscillations filling the probing pulse. The phase difference value u in (1) is defined by the time of spreading the electromagnetic waves to the investigated subject and the sensor:

$$u = 2R_1 \omega_0 / C = 4\pi R_1 / \lambda, \quad (2)$$

where $\omega_0 = 2\pi f_0$ is a circular frequency of the probing signal; f_0 is a mean frequency of the probing signal spectrum; C is a rate of spreading the electromagnetic waves; λ is a wavelength of oscillations filling the probing signal; R_1 is a distance between the investigated subject and the sensor. With the given character of movement of the investigated subject the amplitude $Z(t)$ of the output signal of the correlation system is described by the following expression:

$$Z(t) = E_m \cos(u(t)) \quad (3)$$

where $E_m = (E_0 E_1) / 2 \times n T_0$ is maximum energy of interaction between the return signal and the probing signal, said energy being released at an output load with an unit resistance.

B. Functional diagram of the UWB sensor apparatus for distance measurement

An UWB sensor apparatus whose structural diagram is illustrated in Fig. 2 comprises a microcontroller circuit, a wireless communication interface (Bluetooth), a control circuit, a high-frequency circuit, an UWB antenna and a low-frequency circuit. The timing diagram for signal of the UWB sensor is shown in Fig. 3. Fig. 4 is the UWB sensor not including wireless communication interface (Bluetooth) and a control circuit.

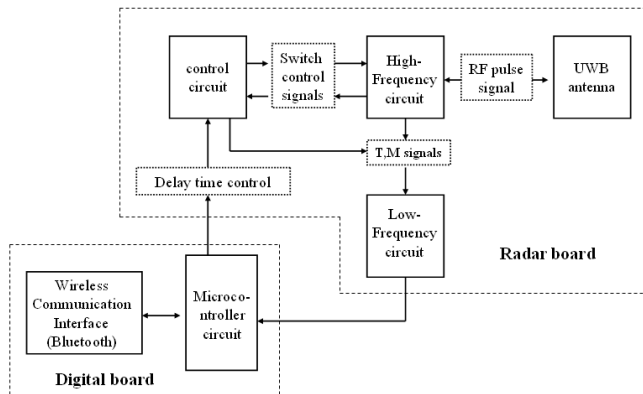


Figure 2. Structure diagram of the UWB sensor apparatus

The microcontroller circuit is used for processing of distance signals, setting of time delay value and transmitting results of measurements via Bluetooth wireless connection. The control circuit is used for determining transmitted and reference RF pulses width w and the value of delay time t_d between transmitted and reference RF pulses. The control circuit has three output signals: oscillator switch control signal (2 on Fig.3), transmit-receive switch control signal (3 on Fig.3) and reference switch control signal (4 on Fig.3), passed to high-frequency circuit. Signals of the control circuit are synchronized by square wave signal with defined period $T_0 = 1/PRF$ (1 on Fig.3), PRF is a pulse repetition frequency.

For a RF pulse generator shown in Fig.4, it is launched by the oscillator switch control signal and forming RF pulses with frequency f , pulse width w_{osc} and period T_0 (5 on Fig.3). In order to decrease amplitudes of oscillator sub-harmonics and low frequency noise spectral components, RF pulse signal is filtered by a RF filter. The output of the RF filter is connected to an input of a RF switch 1. In concordance with the reference switch control signal state, RF pulse signal is transmitted to an RF amplifier 1 to serve as the reference RF pulse signal (7 on Fig.3). Output of the RF switch 1 is connected to a controlled RF switch 2. In concordance with the transmit-receive switch control signal, the controlled RF switch 2 connects an UWB antenna to a RF switch 1 or to a low-noise amplifier 1. The UWB antenna is used for radiation of transmitted RF pulse and reflected RF pulse receiving (8 on Fig.3).

Reflected RF pulse signal is amplified by a low-noise amplifier 1. The output of the low-noise amplifier 1 is connected to RF input of a mixer. The mixer is a phase-shifting circuit providing a phase shift of a reference RF pulse signal. It is M-signal with phase variation. DC signal components on outputs of the mixer are caused by movement of the object changes in the phase incursion of the signal reflected from the investigated subject. The T-signal from counter circuit and the vibration signal (M-signal) are respectively input to the signal processing apparatus, and the proposed algorithm for distance measurement shown in section III is used to perform signal processing analysis to detect a distance between the object and the UWB sensor.

To describe the UWB sensor operation in detail, consider Fig.3 and Fig.4, states of RF switches 1 and 2 define three time intervals of high-frequency circuit operation (Fig.3). During time interval 1, RF switch 1 is connecting RF filter to RF switch 2; RF switch 2 is connecting RF switch 2 to UWB antenna. At that signal of RF pulse generator is amplified by RF switch 2 and transmitted by UWB antenna, thus transmitted RF pulse is formed.

During time interval 2, RF switch 1 is connecting RF filter to RF switch 2; RF switch 2 is connecting UWB antenna to Low-noise amplifier 1. At that phase system does not transmit and does not receive RF pulses. During time interval 3, RF switch 1 is connecting RF filter to RF amplifier 1; RF switch 2 is connecting UWB antenna to Low-noise amplifier 1. Signal of RF pulse generator is amplified by RF amplifier 1 and serves as the reference RF pulse. Reflected RF pulse is

amplified by the Low-noise amplifier 1 and mixed with the reference RF pulse. Thus system has high sensitivity at that time interval.

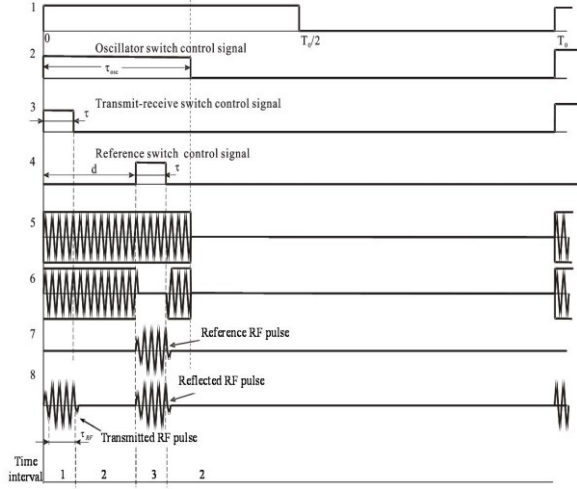


Figure 3. Time diagrams of signal of the UWB sensor

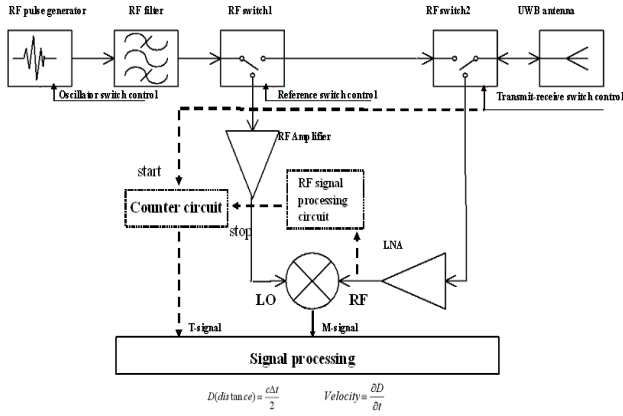


Figure 4. The UWB sensor (not including wireless communication interface and a control circuit)

I. THE PROPOSED ALGORITHM FOR DISTANCE MEASUREMENT

To derive the vibration characteristic for a robot arm of DELTA-type robot, the distance between a robot arm and UWB sensor should be measured. In this section, the proposed algorithm for distance measurement is described. The flowchart illustrating a distance measurement algorithm is shown in Fig. 5.

Refer to Fig. 5, in the first step, a database is created, where the database includes parameters of a distance between the UWB sensor and a robot arm, an output voltage of a mixer, and time of measuring these parameters. Assuming distance measurement experiment between the UWB sensor and the robot arm is performed by M times. The distance between the UWB sensor and the robot arm is d_i , and at a time t_i , the output voltage of the mixer is measured to be V_i . After M times of the distance measurement experiment is performed, the output voltage of the mixer is measured to be V_m^* , where $m=1, 2, \dots, M$. According to voltage measurement results of the M times

of experiments, it is known that at the time t_i , when the distance between the UWB sensor and the robot arm is d_i , an equation of the output voltage V_i is shown as follows:

$$V_i = (V_1^* + \dots + V_M^*)/M. \quad (4)$$

In the second step, when the distance d between the UWB sensor and the robot arm is changed, the corresponding output voltage V can be measured. In this way, a variation trend of the distance d relative to the output voltage V is obtained. According to the variation trend of the measured voltage waveform, the voltage waveform can be divided into L sections. A waveform variation trend of each section can be obtained according to a slope s_l of the waveform curve, so as to determine the variation trend of the distance relative to the output voltage, and an equation of the slope s_l ($l=1, \dots, L$) is as follows:

$$s_l = \frac{\partial V_l}{\partial d_l}. \quad (5)$$

According to a least-square method, a linear regression equation of each waveform segment is obtained, and the equation is as follows:

$$V' = A_l d + B_l, \quad l=1, \dots, L \quad (6)$$

It is assumed that in a section l' , a data sample is $S = \{(d_i, V_i) | i=1, \dots, P\}$, where P is number of data sample. Since the signal is subjected to interference of ambient environment and noise influence, etc., the data sample has N batches of (d_i, V_i) data, where $V_i = V_o$ ($N \ll P$). Now, according to the N batches of data, the corresponding V'_n , $n=1, \dots, N$ are obtained by using the linear regression equation shown in (6). Then, according to a condition of a following equation (7), V'_n with the minimum error value and the corresponding (d_i, V_i) is obtained.

$$\min \|V'_n - V_o\| \quad (7)$$

For the final step, according to the output voltage V of the mixer, and the data sample shown in (8) is obtained in the first and second step, a distance d corresponding to the measurement time t is estimated by using the polynomial interpolation. To calculate d , the polynomial equation should be determined first. Assuming the polynomial equation is (9), based on (10), a_n, \dots, a_0 shown in (9) can be obtained.

$$\tilde{S} = \{(\tilde{d}_i, \tilde{V}_i) | i = 1, \dots, P - N - 1\} \quad (8)$$

$$\tilde{d}_i = a_n \tilde{V}_i^n + a_{n-1} \tilde{V}_i^{n-1} + \dots + a_2 \tilde{V}_i^2 + a_1 \tilde{V}_i + a_0 \quad (9)$$

$$\begin{bmatrix} \tilde{V}_1^n & \tilde{V}_1^{n-1} & \dots & 1 \\ \tilde{V}_2^n & \tilde{V}_2^{n-1} & \dots & 1 \\ \vdots & \vdots & \dots & 1 \\ \tilde{V}_{P-N-1}^n & \tilde{V}_{P-N-1}^{n-1} & \dots & 1 \end{bmatrix} \begin{bmatrix} a_n \\ a_{n-1} \\ \vdots \\ a_0 \end{bmatrix} = \begin{bmatrix} \tilde{d}_1 \\ \tilde{d}_2 \\ \vdots \\ \tilde{d}_{P-N-1} \end{bmatrix} \quad (10)$$

According to (9) that a_n, \dots, a_0 are evaluated from (10), if the output voltage V of the mixer is derived, the distance d between the UWB sensor and a robot arm can be determined.

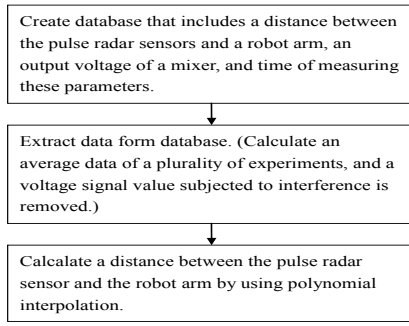


Figure 5. The flowchart for distance measurement algorithm.

II. EXPERIMENTAL SETUP AND RESULTS

To evaluate the performance of our proposed system, the vibration frequency for object and distance signals within a linear stages area are measured. To simulate vibration frequency for object, the vibration signal is generator from function generator. The radar sensors bandwidth is set for the hardware filter range from 0.1 Hz to 100 Hz. Vary the vibration frequencies from 5 Hz to 100 Hz, the frequency correlation for signal measured by UWB sensor and function generator signal is analyzed. The result is shown in Fig. 6. Its x-axis represents frequency measured from UWB with Hz as the unit and the y-axis represents vibration sensing frequency with Hz as the unit. The results indicated that when the frequency is changed from 5 Hz and 100 Hz, the correlation for measured frequency is 1.

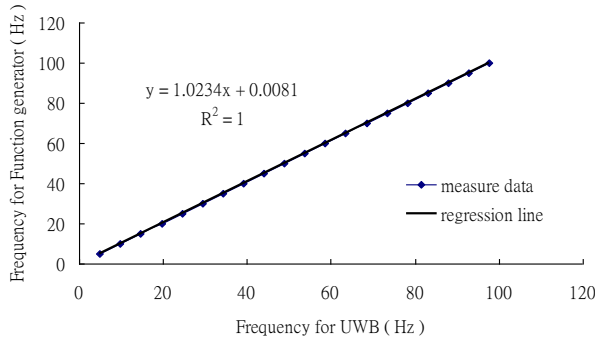


Figure 6. Simulating vibrate linear stages Area. (Frequency)

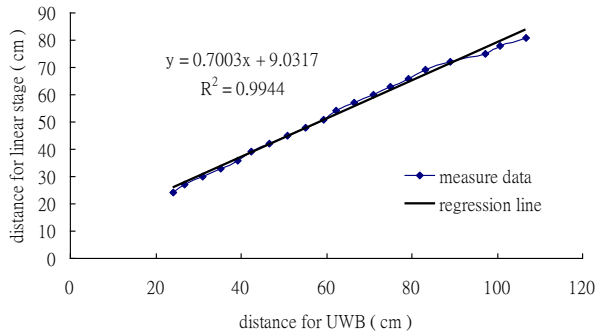


Figure 7. Simulating vibrate linear stages Area. (Distance)

In Fig. 7, the distance correlation for UWB sensor and object moving in linear stage is analyzed. The x-axis shown in Fig. 7 represents the distance measured by UWB sensor with cm as the unit and the y-axis represents the distance measuring from linear stage. The correlation for measured distance from 20 cm and 100 cm is 0.9944.

A calibrated function generator (HP 33120A) and accelerometer (PCB 353B33) were set up to compare with UWB in Fig. 8. Vibration source was controlled by function generator and fixed well with accelerometer. UWB sensor was set up 70 cm away from vibration source and detected the vibration signals at the same time. All the data of UWB were sent to PC via Bluetooth and the data of accelerometer were sent to spectrum analyzer (Agilent 35670A).

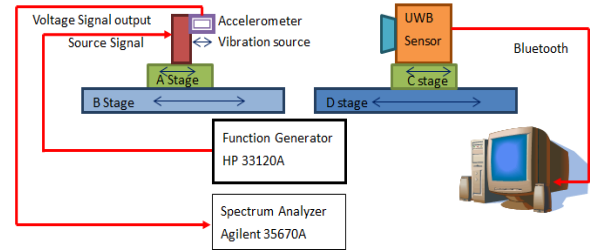


Figure 8. Experimental setup.

We assume this vibration source as the robot arm, and the vibration is usually occurred at low frequency. The vibration source was controlled to vibrate at 3 Hz to 90 Hz and the results measured by accelerometer and UWB was shown in Fig. 9. Then we test the amplitude from 0.02 mm to 1.25 mm, and the result was shown in Fig. 10.

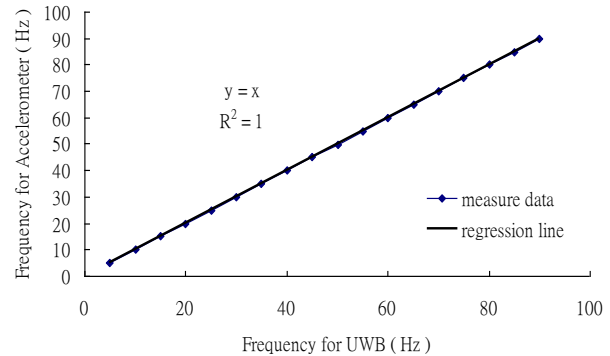


Figure 9. Correlation of frequency between Accelerometer and UWB.

Based on these good correlations between accelerometer and UWB from Fig. 6 to Fig. 10, the performance of our proposed system is acceptable to be used. As long as the vibration signals can be obtained, the system can successfully detect micro-vibration in a linear stages area. In a practical application, the vibration information (i.e. frequency and distance) is the subject to be analyzed to determine whether the vibration signal is a signal from a robot. After the signal is identified, the signal was sent to the control center or feedback to robot slow movement.

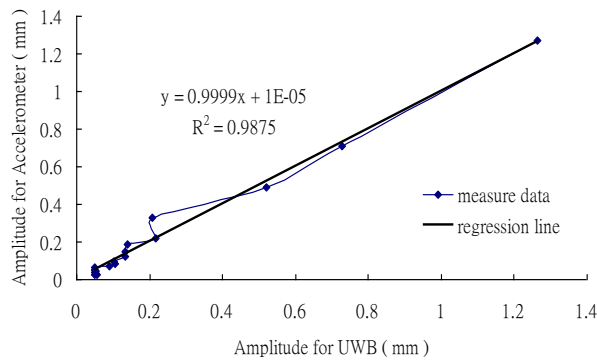


Figure 10. Correlation of amplitude between Accelerometer and UWB.

We also test our UWB sensor to measure real delta-robot which was developed by ourselves. In Fig. 11, the UWB sensor was set 70 cm away from the delta robot and detected the real-time vibration signals. The result was shown in Fig. 12. The signal was symmetrical because the delta robot moving forward and backward. And the UWB was able to detect the vibration signals of delta robot on-line.

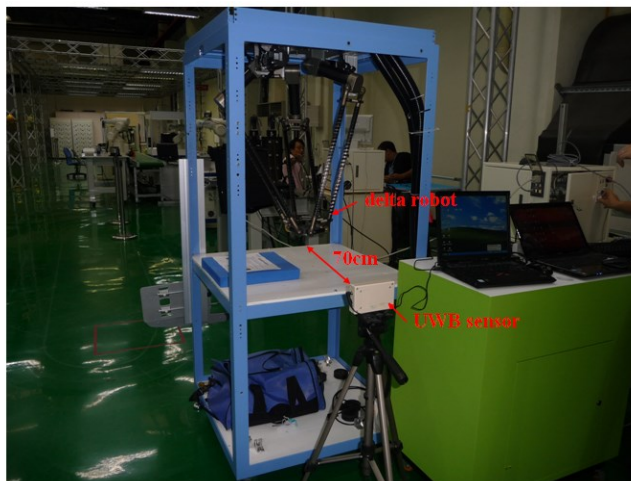


Figure 11. Experimental setup.

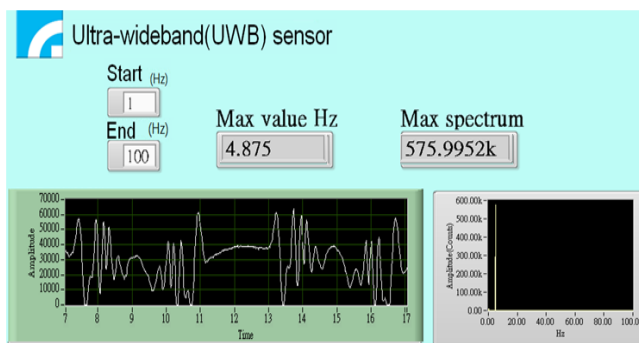


Figure 12. The real-time vibration signals of delta robot measured by UWB.

III. CONCLUSION

An UWB sensor and algorithm to detect vibration and distance of the robot arm are provided. The nature of non-contact measurement makes UWB be more flexible and fewer limitations to apply. The future work for us is to use multiple UWB to proceed with 3D measurement. Not only the vector of vibration signals but also the absolute spatial position might be calculated as real-time information which will help the robots may be controlled more precisely without cost too much. And with non-contact UWB sensor, the quality and throughput of robot arms will be increase because the unwanted or unexpected vibration may be reduced. Furthermore, the UWB can also monitor heart beat information which is related to emotions, health, living wellness and so on. We have worked hard on classifying emotional status and the result is positive. Other respects of research, such as baby and patient monitor, sleeping status monitor, driver's fatigue alarm system, surveillance, culture and creativity applications are proceeding with fine progress. We will reveal our results and aim to promote our advanced UWB sensing technology in the future.

REFERENCES

- [1] Bouri, M. and Clavel, R., "The Linear Delta: Developments and Applications," *Robotics (ISR), 2010 41st International Symposium on and 2010 6th German Conference on Robotics (ROBOTIK)*, pp. 1-8, 2010
- [2] Zhang, Limin, and Song, Yimin M., "Optimal design of the Delta robot based on dynamics," *Robotics and Automation (ICRA), 2011 IEEE International Conference on*, pp. 336-341, 2011
- [3] Park, Hyung-Soon Soon, Chang, Pyung-Hun Hun and Hur, Jong-Sung, "Time-varying input shaping technique applied to vibration reduction of an industrial robot," *Intelligent Robots and Systems, 1999. IROS '99. Proceedings. 1999 IEEE/RSJ International Conference on*, vol. 1, pp. 285-290, 1999
- [4] Harada, Tomoki, Nakamura, Yutaka, Matsumoto, Yosbio and Ishiguro, Horoshi, "Vibration suppression control using a pattern generator for a robot driven by air actuators," *Robotics and Biomimetics, 2008. ROBIO 2008. IEEE International Conference on*, pp. 756-761, 2008
- [5] Furuta, Katsuhisa, Yamakita, Masaki and Sato, Atsushi, "Suppressing vibration of robot arm using frequency-dependent LQ method," *Industrial Electronics, Control and Instrumentation, 1991. Proceedings. IECON '91., 1991 International Conference on*, vol.1, pp. 443-448, 1991
- [6] Xing, Jifeng, Peng, Likun and Lv, Bangjun, "Vibration Reduction of 6-DOF Hydraulic Parallel Robot Based on Robust Control," *Computer and Electrical Engineering, 2008. ICCEE 2008. International Conference on*, pp. 783-788, 2008
- [7] Kostić, Dragan, De Jager, Bram and Steinbuch, Maarten, "Robust attenuation of direct-drive robot-tip vibrations," *Intelligent Robots and Systems, 2002. IEEE/RSJ International Conference on*, vol. 3, pp. 2206-2212, 2002
- [8] Choi, Sang, Fuhlbrigge, Thomas A. and Nidamarthi, Srinivas, "Vibration analysis in robotic ultrasonic welding for battery assembly," *Automation Science and Engineering (CASE), 2012 IEEE International Conference on*, pp. 550-554, 2012
- [9] Krauss, Ryan W. and Book, Wayne J., "Stability in active mass damping control of a flexible robot," *Aerospace Conference, 2004. Proceedings. 2004 IEEE*, vol.5, pp. 2903-2911, 2004
- [10] Igor Y. Immoreev, Sergey Samkov and Teh-Ho Tao, "Short - Distance Ultrawideband Radars," *Aerospace and Electronic Systems Magazine, IEEE*, Vol. 20, Issue 6, pp.9-14., 2005